Desalination and Water Treatment
www.deswater.com

46 (2012) 124–138
August

1944-3994/1944-3986 © 2012 Desalination Publications. All rights reserved
doi: 10.1080/19443994.2012.677412

Taylor & Francis
Taylor & Francis Group

Verification of double-shell model for sorption of cesium, cobalt, and europium ions on poly-acrylonitrile-based Ce(IV) phosphate from aqueous solutions

B. El-Gammal[a,]*, S.S. Metwally[a], H.F. Aly[a], S.A. Abo-El-Enein[b]

[a]*Hot Laboratories Center, Atomic Energy Authority, Post Code 13759, Cairo, Egypt*
Tel./Fax: +20 222060107; e-mail: belalelgammal@hotmail.com
[b]*Faculty of Science, Chemistry Department, Ain Shams University, Cairo, Egypt*

Received 6 August 2011; Accepted 7 February 2012

ABSTRACT

Kinetic and equilibrium models were navigated for sorption of Cs^+, Co^{2+}, and Eu^{3+} ions from their aqueous solutions by poly-acrylonitrile-based Ce(IV) phosphate. Pseudo-first order, pseudo-second order, intra-particle diffusion, and Boyed rate expressions were used to determine the suitable sorption pathway, in addition to their verification using the double-shell theory. Such expressions initially revealed that the sorption process is governed by the pseudo-second-order and particle diffusion protocols; DSM finally confirmed that chemical reaction and/or film diffusion control could be discarded as controlling steps. Langmuir and Freundlich isotherm models were applied and separately compared. Thermodynamic parameters were determined. Positive values of enthalpy change, ΔH (27.5, 28.2, and 29.1 kJ/mol), for Cs^+, Co^{2+}, and Eu^{3+} ions confirmed the endothermic nature of the sorption process and suggested that chemisorption was the predominant mechanism. The high positive values of the entropy change, ΔS (142.77, 123.10, and 118.19 J/mol/K) for the mentioned cations, showed an increased randomness at the solid/solution interface. The obtained negative values of free energy change, ΔG (−8.4 to −12.28, −4.88 to −7.951, and −3.743 to −6.757 kJ/mol), for the aforementioned species indicated the feasibility and the spontaneous nature of the sorption at different reaction temperatures.

Keywords: Ion exchange; Acrylonitrile; Cerium(IV) phosphate; Cesium; Cobalt and europium

---

1. Introduction

Removal of large amounts of various cations, including radioactive ^{137}Cs, ^{60}Co, and $^{152+154}Eu$ and highly toxic Cs^+, Co^{2+}, and Eu^{3+} cations, from the environment and nuclear wastes is a subject of significant interest due to the hazards they pose. Radioactive ^{137}Cs, ^{60}Co, and $^{152+154}Eu$ ions are significant components of nuclear waste and nuclear fallout [1]. For example, in the Hanford site (located in Washington State and operated by the U.S. Department of Energy), 53 million gallons of high-level radioactive wastes are currently stored in 177 underground steel tanks [2]. Some of these tanks are known to have leaked [2], and the waste is still waiting for final disposition. A significant component of radioactivity in spent nuclear fuel arises from ^{137}Cs, ^{60}Co, and $^{152+154}Eu$ [3]. Especially ^{137}Cs is often a component of dirty bombs and presents a serious threat, both to the environment and to human beings, as a result of its relatively long half-life

---

*Corresponding author.

($T_{1/2}$ = ~30 years), high solubility/mobility (up to 186, 209, 261, and 400 g/100 g of water at ~20°C for CsCl, $CsHCO_3$, Cs_2CO_3, and CsOH, respectively, and strong-emitting radiation [4]. A wide range of ion-exchange materials are available for the treatment of ^{137}Cs, ^{60}Co, and $^{152+154}$Eu. These materials are available in a variety of forms, having widely differing chemical and physical properties. They may be classified as naturally occurring or synthetic. In this study, a composite material that possesses a fibrous structure was used as ion exchanger for the removal of simulated ^{137}Cs, ^{60}Co, and $^{152+154}$Eu ions from aqueous solutions. The introduction of a polymeric species into an inorganic fibrous material greatly enhances its mechanical strength and gives a good ion-exchange capacity [5]. Therefore, poly-acrylonitrile-based cerium(IV) phosphate was tried as an adsorbent in this study.

2. Materials and methods

2.1. Chemicals and reagents:

All chemicals and reagents were of analytical reagent grade and were used without further purification. Nitric acid [HNO_3] was obtained from Porlabo, europium chloride [$EuCl_3$] from Aldrich Chem. Co., and cobalt chloride [$CoCl_2$] and cesium chloride [CsCl] were purchased from Merck. The pH was adjusted by the addition of NH_4OH which was obtained from Fluka. For all experiments, double-distilled water was used as the main solvent. However, the different chemicals and reagents were prepared by dilution and standardized by suitable analytical methods.

2.2. Apparatus:

A Shimadzu UV–visible spectrophotometer model UV-160 A, Japan was used for the determination of europium. Atomic absorption spectrophotometer (Buck Scientific) model 210 VGP, USA, was used to analyze cobalt and cesium ions in the solution. For batch investigation, a good shaking for the two phases was achieved using a thermostatic mechanical shaker. The hydrogen ion concentration of different solutions was measured using Schott Gerate CG 820 pH meter, Germany.

2.3. Adsorption studies

The batch technique was employed by shaking 50 mL test tubes containing 0.05 g of poly-acrylonitrile-based Ce(IV) phosphate with 10 mL of 10^{-4} mol/L metal ion solution of Cs^+, Co^{2+}, and Eu^{3+}, adjusting the pH at 2, for 4 h to attain equilibrium at room temperature. The suspension obtained was centrifuged to separate the solid from the liquid phase. The clear aqueous phases obtained were diluted to an appropriate concentration range for the elemental analysis using atomic absorption spectrophotometer and UV–visible spectrophotometer. The quantity sorbed of metal ion, q_e, can be calculated from the following equation:

$$q_e = (C_0 - C_e) \times \frac{V}{m} \tag{1}$$

where q_e is the quantity sorbed of metal ion at equilibrium (mmol/g), C_0 and C_e are the initial and equilibrium metal ion concentration respectively (mmol/L), V is the volume of the sample (L), and m is the weight of the adsorbent (g).

2.4. Kinetic studies:

Kinetic studies were performed at various temperatures of 298, 303, 313 and 323 K, and 10^{-4} mol/L of metal ion concentration. The experiments were also conducted at different concentrations, 10^{-2}–10^{-4} mol/L of Cs, Co, and Eu ions at room temperature. For these investigations, 0.05 g of poly-acrylonitrile derived Ce(IV) phosphate was mixed with a 10 mL solution containing the known concentrations of Cs^+, Co^{2+}, and/or Eu^{3+} ions and the solutions in different stoppered bottles were shaken in a thermostat shaker. The samples were measured, as a function of time, by separating the liquid phase and its concentration was measured.

3. Results and discussion

3.1. Effect of pH:

The effect of pH in the range from 1 to 8 on the distribution coefficient of 10^{-4} mol/L Cs^+, Co^{2+}, and Eu^{3+} ions by poly-acrylonitrile-based Ce(IV) phosphate was investigated. Fig. 1 represents a relation between the logarithm of the distribution coefficients, $\log K_d$ and pH values. It was observed that each metal ion sorption process is dependent on the initial pH of the solution and the distribution coefficient of ions sorbed increased with an increase in the pH value. At lower values, the distribution coefficient was inhibited in this acidic medium, and this can be attributed to the presence of H^+ ions competing with the Cs^+, Co^{2+}, and/or Eu^{3+} ions for the sorption sites. The distribution coefficient continuously increases with the

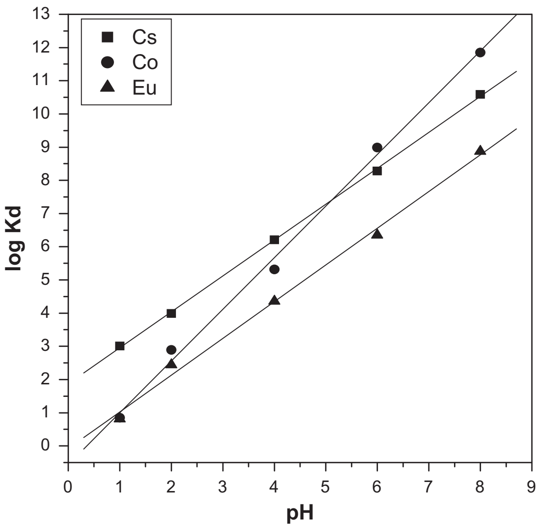

Fig. 1. Effect of pH on distribution coefficient of 10^{-4} M Cs^+, Co^{2+} and Eu^{3+}.

increase in pH value and the highest uptake was observed at pH range from 6.0 to 8.0. This figure gives straight lines with slope 1.16 for Cs and 1.55 for Co, which investigate the valence [6,7], according to the following equation:

$$\mathrm{Log}K_\mathrm{d} = \mathrm{Log}K_\mathrm{ex}[\overline{R - H^+}]^n + npH \quad (2)$$

The plot of Log K_d against pH gives a straight line with slope equal to n, which represents the number of hydrogen ions released and corresponding to the valency of metal ion, this is applicable to Cs^+ and Co^{2+} ions, but differs in the case of Eu^{3+} ion, with slope equal to 1.13, since at higher pH values, the uptake of trivalent Eu^{3+} ions was slightly decreased, which may be attributed to the variation of the chemical species, due to the formation of the hydroxide complexes of Eu ions ($Eu(OH)^{2+}$ and $Eu(OH)_2{}^+$) in solution [8].

3.2. Effect of contact time and temperature

Fig. 2 represents the plot of percent uptake of 10^{-4} M Cs^+, Co^{2+}, and Eu^{3+} ions vs. contact time to illustrate the effect of contact time on the uptake of aforementioned ions by using poly-acrylonitrile-based Ce(IV) phosphate as a cation exchanger from aqueous solution of 0.01 M HNO_3 batchwise at room temperature. The percent uptake sharply increases at the initial stages by increasing the shaking time until the equilibrium is obtained, 97.50% for Cs, 79.49 for Co, and 58.1 for Eu ions as shown in Fig. 2. Table 1 illustrates that the time required for equilibrium is within 60 min for Cs, 90 min for Co and Eu ions. Plotting the amount adsorbed, q, vs. time for the adsorption of the ions at different temperatures of 298, 303, 313, and 323 K is indicated by Figs. 3–5 respectively, which illustrate that the amount adsorbed increases with increasing temperature. This increase indicates the endothermic nature of the adsorption process of Cs^+, Co^{2+}, and Eu^{3+} onto a poly-acrylonitrile-based Ce(IV) phosphate resin.

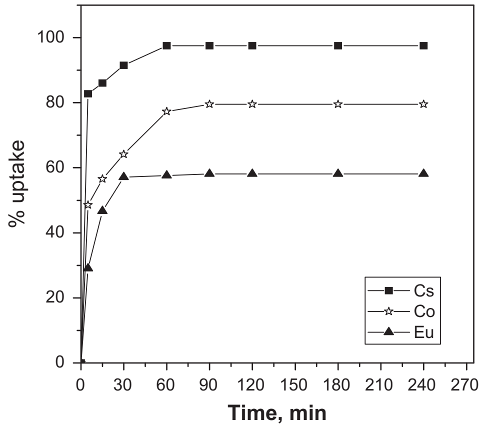

Fig. 2. Effect of contact time on uptake of Cs, Co and Eu ions.

3.3. Adsorption kinetics modeling [9,10]

$$\mathrm{Log}(q_\mathrm{e} - q_t) = \mathrm{Log}q_\mathrm{e} - \frac{k_1}{2.303}t \quad (3)$$

The value of pseudo-first-order rate constant, k_1, and the amounts adsorbed at equilibrium, q_e, value can be determined by plotting Log($q_\mathrm{e} - q_t$) against t, as shown in Figs. 6–8. These figures give straight lines; from the slope and intercept, one can determine the values of k_1 and q_e. Table 1illustrates the values of k_1, q_e, and R^2. As can be seen from the three figures and the table, despite the correlation coefficients for the pseudo-first-order kinetic model obtained at 298, 303, 313, and 323 K for the three metal ions, under study, being quite high, the calculated q_e values do not give reasonable values, and are not close to the experimental values, so the adsorption of Cs, Co, and Eu ions on poly-acrylonitrile-based Ce(IV) phosphate resin does not fit into this equation.

The second model used to describe the kinetics of the adsorption of Cs^+, Co^{2+}, and Eu^{3+} ions onto poly-acrylonitrile-based Ce(IV) phosphate at different temperatures is the pseudo-second-order model, which is demonstrated in Eqs. (4) [11] as

Table 1
Kinetic parameters for pseudo-first-order adsorption of Cs+, Co^{2+} and Eu^{3+} at different temperature

Temperature (K)	Cs				Co				Eu			
	k_1 (min^{-1})	q_e (exp. mmol/g)	q_e (calc., mmol/g)	R^2	k_1 (min^{-1})	q_e (exp. mmol/g)	q_e (calc., mmol/g)	R^2	k_1 (min^{-1})	q_e (exp. mmol/g)	q_e (calc., mmol/g)	R^2
298	0.037	0.0,195	0.0,037	0.983	0.066	0.0,033	0.0,020	0.959	0.076	0.0,133	0.0,064	0.858
303	0.036	0.0,196	0.0,033	0.973	0.063	0.0,035	0.0,016	0.953	0.039	0.0,145	0.0,061	0.963
313	0.035	0.0,198	0.0,030	0.999	0.047	0.0,037	0.0,009	0.989	0.038	0.0,161	0.0,067	0.995
323	0.032	0.0,199	0.0,026	0.995	0.046	0.0,039	0.0,007	0.979	0.030	0.0,174	0.0,024	0.915

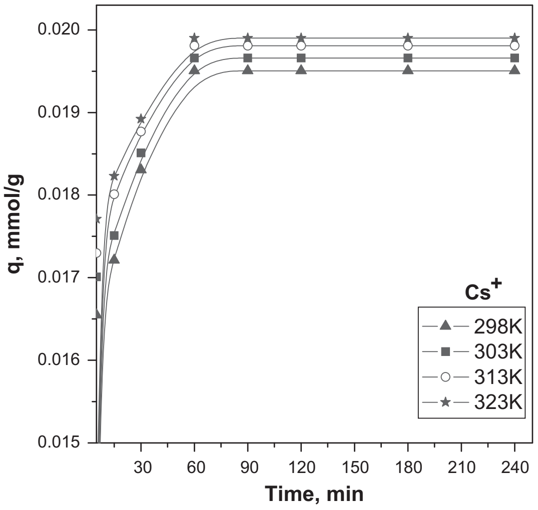

Fig. 3. Effect of contact time on quantity sorbed of Cs^+ ion.

$$\frac{t}{q} = \frac{1}{k_2 q_e^2} + \frac{1}{q_e} t \tag{4}$$

The pseudo-second-order parameters values can be determined from the slope, and the intercept of the plots of t/q vs. t, respectively. Figs. 9–11 give straight lines from which one can determine the values of k_2 and q_e. Table 2 illustrates that the calculated q_e values are closer to the experimental data than the calculated values of the pseudo-first-order model, and the correlation coefficients are very high, $R^2 > 0.98$, for pseudo-second-order kinetic model. Therefore, the adsorption of the three metal ions can be approximated more

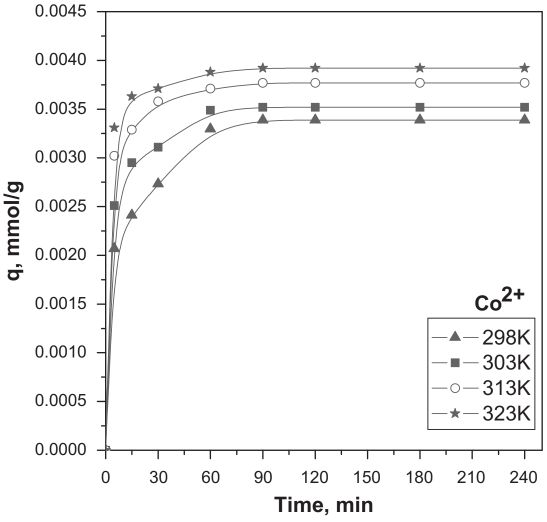

Fig. 4. Effect of contact time on quantity sorbed of Co^{2+} ion.

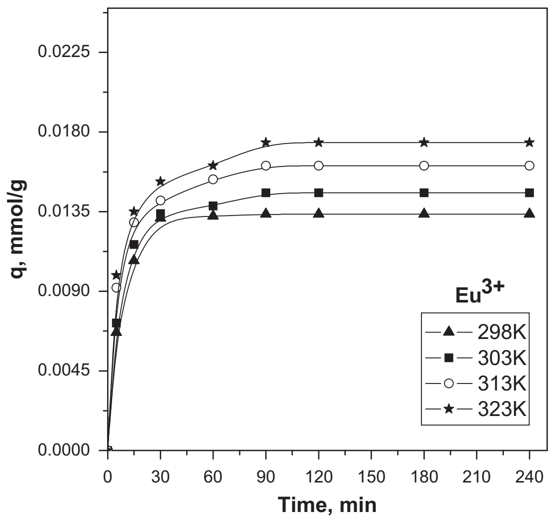

Fig. 5. Effect of contact time on quantity sorbed of Co^{2+} ion.

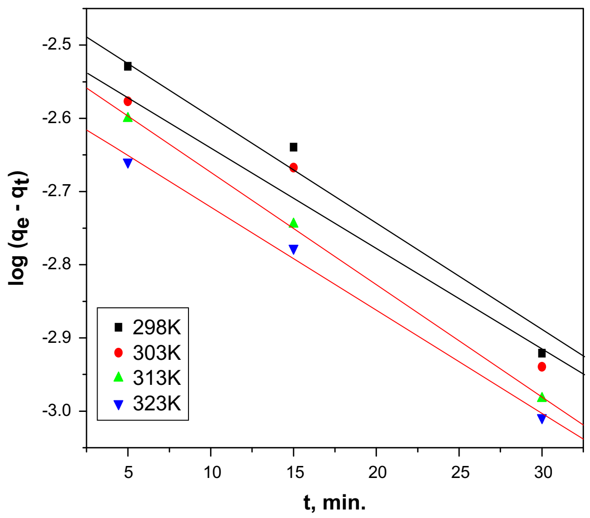

Fig. 6. Pseudo-first-order plots for sorption of Cs + at different temperatures.

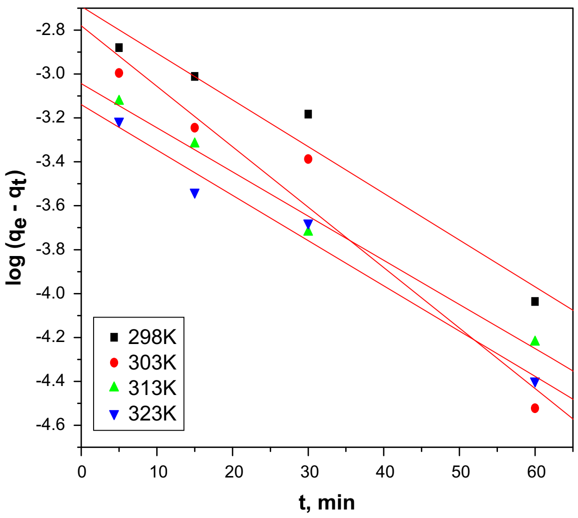

Fig. 7. Pseudo-first-order plots for sorption of Co^{2+} at different temperatures.

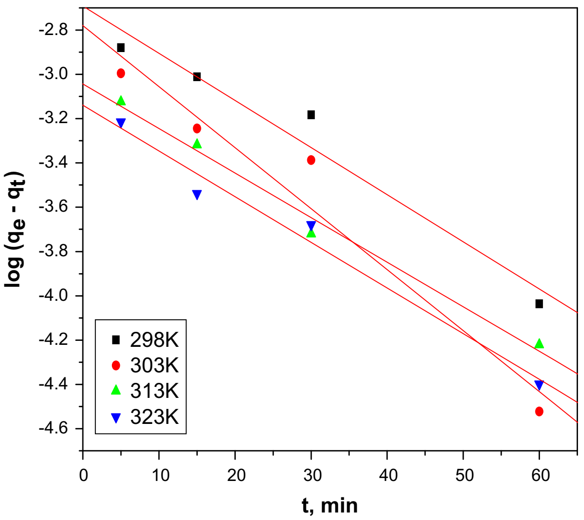

Fig. 8. Pseudo-first-order plots for sorption of Eu^{3+} at different temperatures.

favorably by the pseudo-second-order model thus reinforcing the applicability of this model.

The three following steps are thought to be involved during the adsorption of any organic or inorganic substance over the surface of a porous adsorbent [12]: transport of adsorbate to the surface of the adsorbent (film diffusion), transport of the adsorbate within the pores of the adsorbent (particle diffusion), and adsorption of the adsorbate on the interior surface of the adsorbent.

Out of these three processes, the third step is quite rapid, which cannot be treated as the rate-determining step [13].

Intra-particle diffusion model assumes that the film diffusion is negligible and intra-particle diffusion is the rate-controlling step, which is usually true for well-mixed solutions [14]. The intra-particle diffusion model, Morris and Weber model, could be presented as follows:

$$q = k_{\mathrm{ad}} * t^{1/2} + C \qquad (5)$$

where k_{ad} is the rate constant of intra-particle transport (mmol/g min$^{1/2}$). The value C (mmol/g) in this equation is a constant, which indicates that there

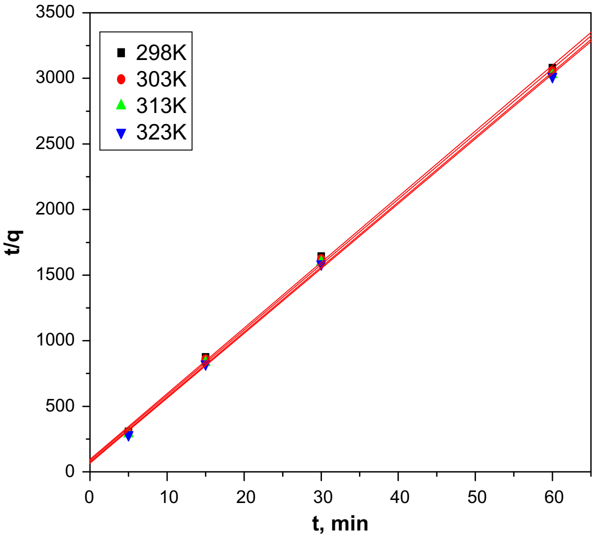

Fig. 9. Pseudo-second-order plots for sorption of Cs^+ at different temperatures.

exists a boundary layer diffusion effects and is proportional to the extent of boundary layer thickness [15]. The larger the value, the greater is the boundary effect. The plots of q vs. $t^{1/2}$ are given in Figs. 12–14 for the adsorption of Cs, Co, and Eu ions, respectively, onto poly-acrylonitrile-based Ce(IV) phosphate resin at different temperatures. It can be seen from the figures that the adsorption data give a straight lines; therefore, the adsorption process is controlled by intra-particle diffusion. Table 3 gives the kinetic parameters for this model.

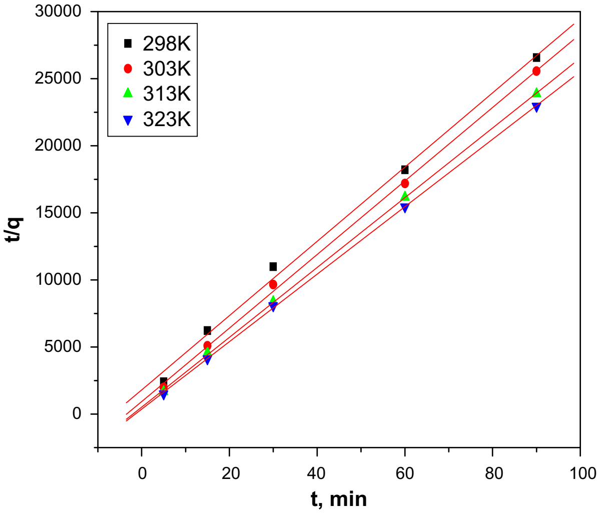

Fig. 10. Pseudo-second-order plots for sorption of Co^{2+} at different temperatures.

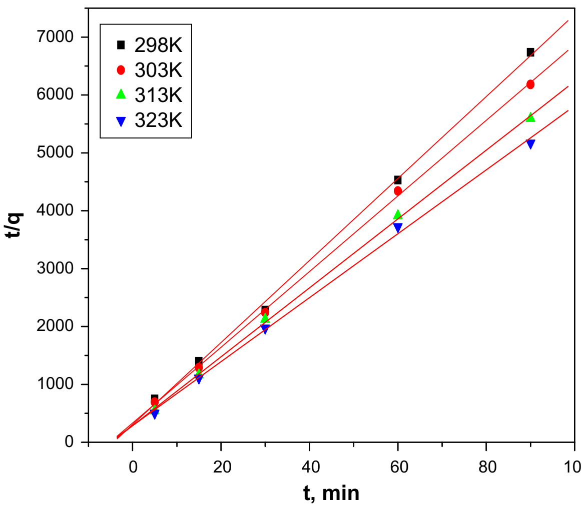

Fig. 11. Pseudo-second-order plots for sorption of Eu^{3+} at different temperatures.

In order to identify the step governing the overall removal rate of the sorption process, the model given by Boyd et al. [16] was applied. In this model, various parameters were calculated using the following expressions:

$$F = 1 - \left(\frac{6}{\pi^2}\right) \sum_{n=1}^{\infty} \frac{1}{n^2} \exp^{(-nBt)} \tag{6}$$

where F is the fractional attainment of equilibrium at time t ($F = q_t/q_e$), n is an integer number 1, 2, or 3, and B is a mathematical function equal:

$$B = \pi^2 D_i / r^2 \tag{7}$$

where D_i is the effective diffusion coefficient of metal ion, r^2 is the radius of the solid particle $[(0.5 \times 0.05)^2]$. According to Boyd equation, F is a function of (B) and (t) only, and thus is independent of the external solution. Experimental results may be tested to determine whether they confirm the above equation by plotting the values of (Bt) against the corresponding values of (t) where (Bt) values are taken from Reichenberg's table [17] as follows:

$$Bt = -0.4,977 - \ln(1 - F) \tag{8}$$

The linearity test of Bt vs. time plots is employed to distinguish the film and particle diffusion-controlled rates of the sorption process. If the plot is a straight line passing through the origin, then the sorption rate is governed by the particle diffusion mechanism, otherwise it is governed by film diffusion [18].

Table 2
Kinetic parameters for pseudo-second-order adsorption

Temperature (K)	Cs			Co			Eu		
	k_2 (g/mmol/min)	q_e (calc., mmol/g)	R^2	k_2 (g/mmol/min)	q_e (calc., mmol/g)	R^2	k_2 (g/mmol/min)	q_e (calc., mmol/g)	R^2
298	0.439	0.01,997	0.999	0.707	0.00,361	0.996	0.273	0.014	0.998
303	0.480	0.02,008	0.999	1.337	0.00,365	0.999	0.213	0.015	0.999
313	0.554	0.02,017	0.999	2.147	0.00,384	0.999	0.205	0.017	0.999
323	0.615	0.02,022	0.999	2.875	0.00,397	0.999	0.177	0.018	0.998

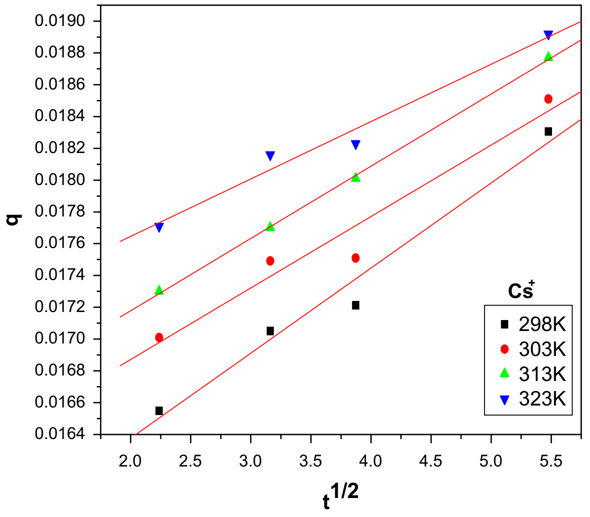

Fig. 12. Intra-particle diffusion model for Cs^+ at different temperatures.

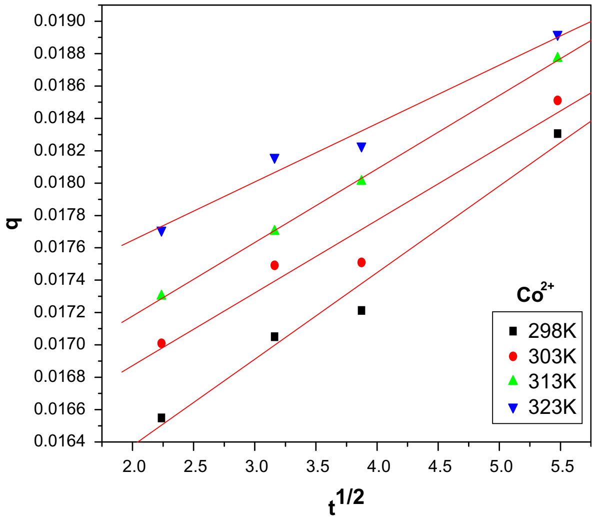

Fig. 13. Intra-particle diffusion model for Co^{2+} at different temperatures.

Figs. 15–17 depict the *Bt* vs. time plots for Cs^+, Co^{2+}, and Eu^{3+}, respectively, at different temperatures. The plots are linear passing through the origin for the three metal ions, indicating that the particle diffusion is the controlled rate of sorption process at all studied temperatures. The values of D_i calculated at different studied temperatures for the ions are presented in Table 4. For physical adsorption, the value of the effective diffusion coefficient ranges from 10^{-6} to $10^{-9}\,m^2/s$ and for chemisorption, the value ranges from 10^{-9} to $10^{-17}\,m^2/s$ [19]. The difference in the values is due to the fact that in physical adsorption the

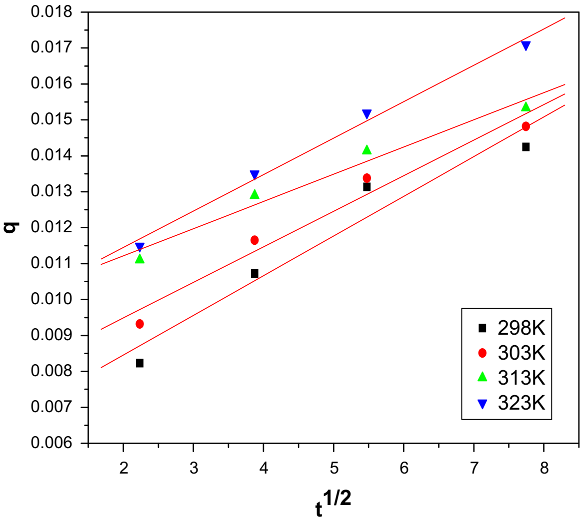

Fig. 14. Intra-particle diffusion model for Eu^{3+} at different temperatures.

molecules are weakly bound and therefore there is an ease of migration, whereas for chemisorption the molecules are strongly bound and mostly localized. The obtained values of D_i were of the order of $10^{-12}\,m^2/s$ for Cs and Co ions and 10^{-13} for Eu ion, indicating the chemisorption nature of sorption process. Plotting of $\ln D_i$ vs. $1/T$ gave straight lines, as shown in Fig. 18 which proves the validation of the linear form of Arrhenius equation:

$$\ln D_i = \ln D_o - E_a/RT \qquad (9)$$

where D_o is a pre-exponential constant analogous to Arrhenius frequency factor. The energies of activation for all ions, E_a, were calculated from the slope of the straight lines, the obtained values presented in Table 4. The values of E_a below 42 kJ/mol generally indicate diffusion-controlled processes and higher values represent the chemical reaction processes [20,21].

Such a low value of the activation energy for the sorption of each metal ion indicates a chemical sorption process involving weak interaction between sorbent and sorbate and suggests that each sorption process has a low potential energy.

According to Marcus, as the porosity of the polymer is apparently small and thus practically impermeable to the fluid reactant, the sorption process may be interpreted by the ''Double-Shell Progressive'' approach, that can be depicted in terms of the concentration profile of a liquid reactant containing a solute accelerating into a spherical bead of a partially saturated sorbent. The description of the rate of sorption

Table 3
The kinetic parameters for intra-particle diffusion model for adsorption of Cs^+, Co^{2+} and Eu^{3+}

Temperature (K)	Cs			Co			Eu		
	k_{ad} (mmol/g min$^{1/2}$)	C (mmol/g)	R^2	k_{ad} (mmol/g min$^{1/2}$)	C (mmol/g)	R^2	k_{ad} (mmol/g min$^{1/2}$)	C (mmol/g)	R^2
298	5.35×10^{-4}	0.01,531	0.989	2.2×10^{-4}	0.0,016	0.997	1.10×10^{-3}	0.0,063	0.940
303	4.49×10^{-4}	0.01,597	0.952	1.7×10^{-4}	0.0,022	0.971	9.89×10^{-4}	0.0,075	0.965
313	4.34×10^{-4}	0.01,627	0.999	1.3×10^{-4}	0.0,028	0.944	7.58×10^{-4}	0.0,097	0.971
323	3.61×10^{-4}	0.01,693	0.976	9.7×10^{-5}	0.0,032	0.914	1.01×10^{-4}	0.0,099	0.992

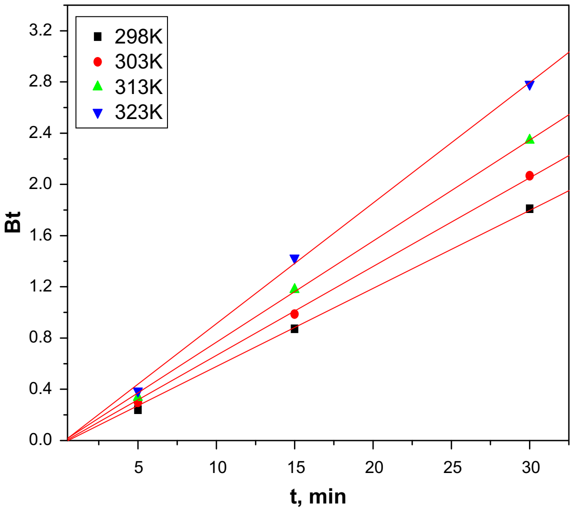

Fig. 15. Plot of *Bt* vs. time for the sorption of Cs^+ ion at different temp.

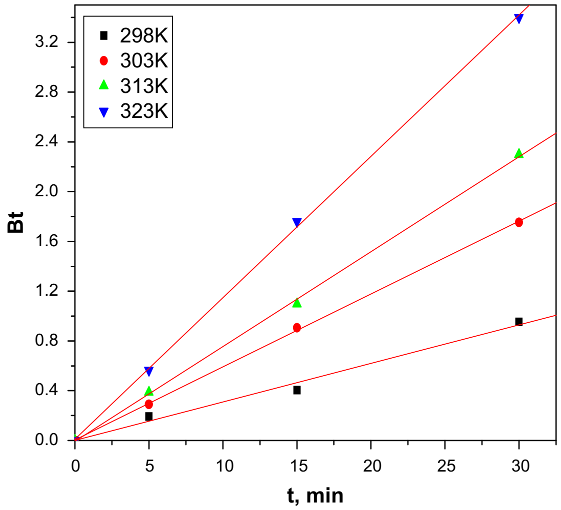

Fig. 16. Plot of *Bt* vs. time for the sorption of Co^{2+} ion at different temp.

according to a shell-core mechanism might also be valid for species with a high affinity for the resin, resulting in quasi-irreversible sorption. According to later discussed Langmuir and Freundlich models, the tested solutes have large binding constants on the used composites. Therefore, attempts were made to fit sorption kinetic data to shell-core models. In this case, the relationship between sorption time and degree of sorption is given by the following expressions [22,23].

As the fluid film controls,

$$F = \frac{3C_{Ao}k_{mA}}{arC_{so}}t \tag{10}$$

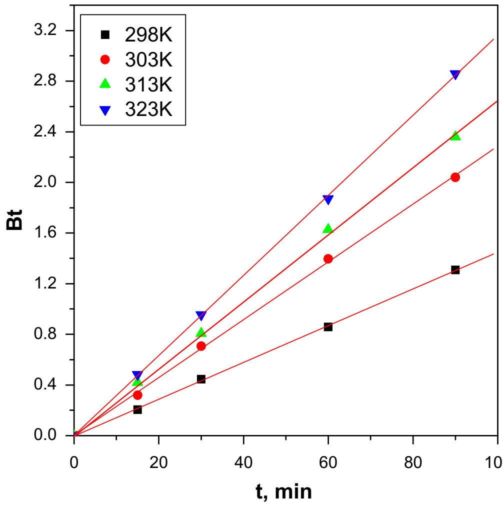

Fig. 17. Plot of *Bt* vs. time for the sorption of Eu^{3+} ion at different temp.

When the diffusion though the sorption layer controls,

$$\left[3 - 3(1-F)^{2/3} - 2F\right] = \frac{6D_eC_{Ao}}{ar^2C_{so}}t \tag{11}$$

Finally, as the chemical reaction controls,

$$\left[1 - (1-F)^{1/3}\right] = \frac{k_sC_{Ao}}{r}t \tag{12}$$

where C_{Ao} is the molar concentration of sorbing species A in bulk solution, while C_{so} represents their concentration at the bead's unreacted core, k_{mA} is the mass transfer coefficient of species A through the liquid film in m/s, a is a stoichiometric coefficient, r is the average particle radius in m, D_e is the diffusion coefficient in solid phase in m^2/s, and k_s is the reaction constant based on surface in m/s.

Figs. 19–21 show the results of the different Cs^+, Co^{2+}, and Eu^{3+} sorption kinetics in the light of the three previous equations. They indicate that the chemical reaction and/or film diffusion control can be discarded as controlling steps, since they did not give straight-line profiles. Both the Boyed and the shell progressive models describe the experimental data satisfactorily over the entire time range. A relatively good straight line could also be obtained for the film diffusion model over a shorter range, especially for europium sorption on the composite.

3.4. Sorption isotherms

In this study, the relationship between the adsorbed and the aqueous concentrations at equilib-

Table 4
Diffusion coefficient for the sorption of Cs^+, Co^{2+} and Eu^{3+} onto poly-acrylonitrile based Ce(IV) phosphate

Temperature (K)	D_i (m^2/s)			D_o (m^2/s)			E_a (kJ/mol)		
	Cs	Co	Eu	Cs	Co	Eu	Cs	Co	Eu
298	3.89×10^{-12}	1.96×10^{-12}	9.20×10^{-13}	9.0×10^{-6}	6.3×10^{-6}	5.0×10^{-6}	29.65	30.05	31.9
303	4.45×10^{-12}	3.72×10^{-12}	1.45×10^{-12}						
313	5.04×10^{-12}	4.83×10^{-12}	1.67×10^{-12}						
323	6.15×10^{-12}	5.20×10^{-12}	2.00×10^{-12}						

rium has been described by three isotherm models; Freundlich, Langmuir, and Dubinin–Radushkevich.

Langmuir isotherm is valid for monolayer adsorption onto a surface containing a finite number of identical sites. It is characterized by a decreasing slope as the concentration increases, since vacant adsorption sites decrease as the adsorbent becomes covered. Langmuir adsorption equation can be expressed as:

$$\frac{1}{q_e} = \frac{1}{Q} + \frac{1}{bQ} * \frac{1}{C_e} \tag{13}$$

where C_e is the equilibrium concentration (mmol/L), q_e is the amount of solute adsorbed per unit weight of adsorbent (mmol/g) at equilibrium time, Q is the monolayer adsorption capacity (mmol/g), and b is the constant related to the free energy of adsorption ($b \alpha e^{-\Delta G/RT}$). Applying Langmuir isotherm by plotting $1/C_e$ against $1/q_e$ as shown in Figs. 22–24 for Cs, Co, and Eu, respectively, straight lines are obtained for the three ions, confirming that this expression is indeed a reasonable representation of the chemisorption isotherm. From the slope and intercept, one can determine the Langmuir constants as shown in Table 5. The monolayer sorption capacity (Q) for the three ions was found to be increased with temperature, showing that the sorption capacity is enhanced at higher temperatures. This increase in sorption capacity with temperature suggested that the active surfaces available for sorption have increased with temperature. Another reason may be due to the change in pore size and the enhanced rate of intra-particle diffusion of solute, as diffusion is an endothermic process [24].

Freundlich equation can be expressed as follows:

$$\log q_e = \frac{1}{n} \log C_e + \log k \tag{14}$$

By plotting $\log q_e$ against $\log C_e$, straight lines were obtained for the adsorption of the three metal ions on poly-acrylonitrile-based cerium(IV) phosphate from 0.01 M HNO_3 medium at different temperatures, as

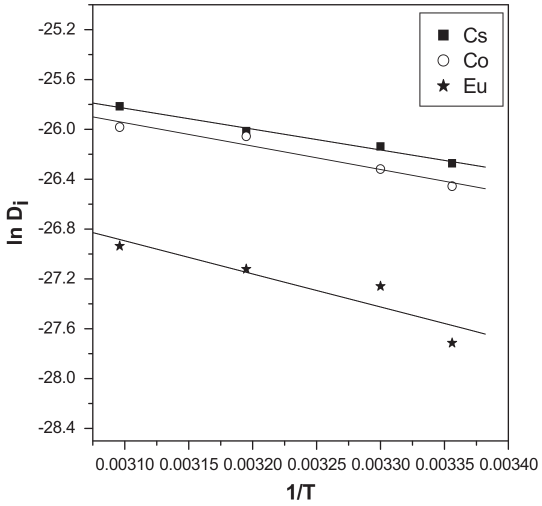

Fig. 18. Arrhenius plot for the particle diffusion coefficients of Cs, Co and Eu ions.

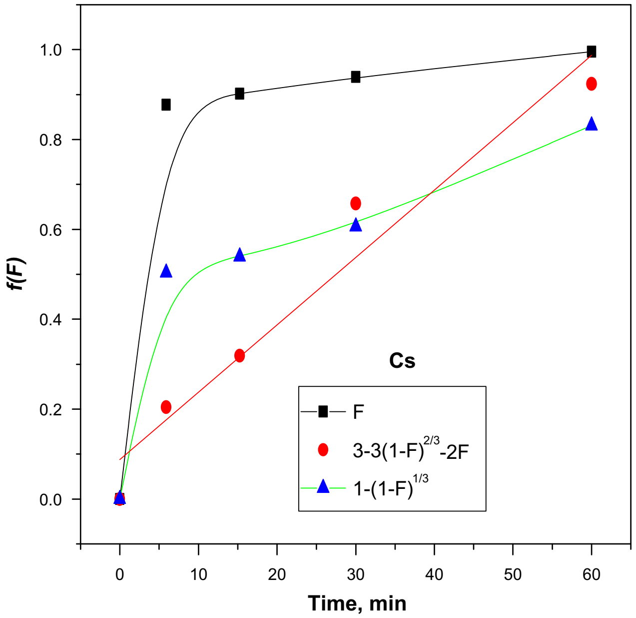

Fig. 19. Verification of the double shell model for Cs^+ adsorption.

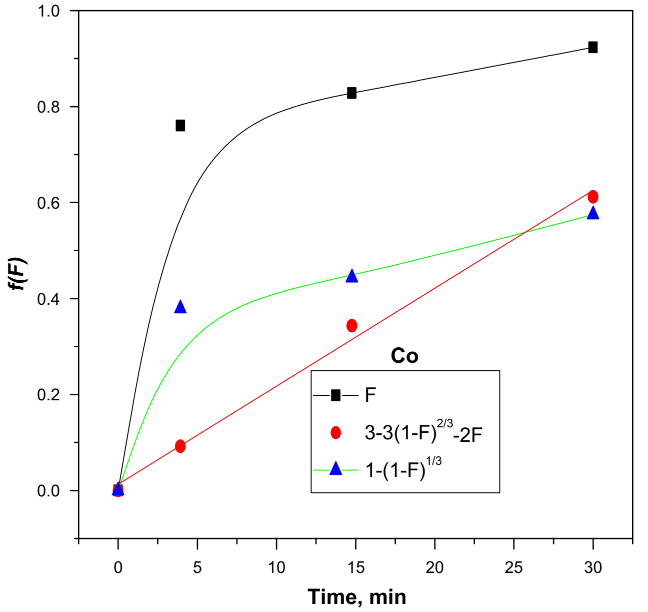

Fig. 20. Verification of the double shell model for Co^{2+} adsorption.

presented in Figs. 25–27. From the slope, one can determine the Freundlich constants, k and n, where k is an indicator to the strength of adsorption bond and n is as exponent constant related to the adsorption intensity or bond distribution and its values are less than 1, indicating a concentration-dependent parameter, as shown in Table 6.

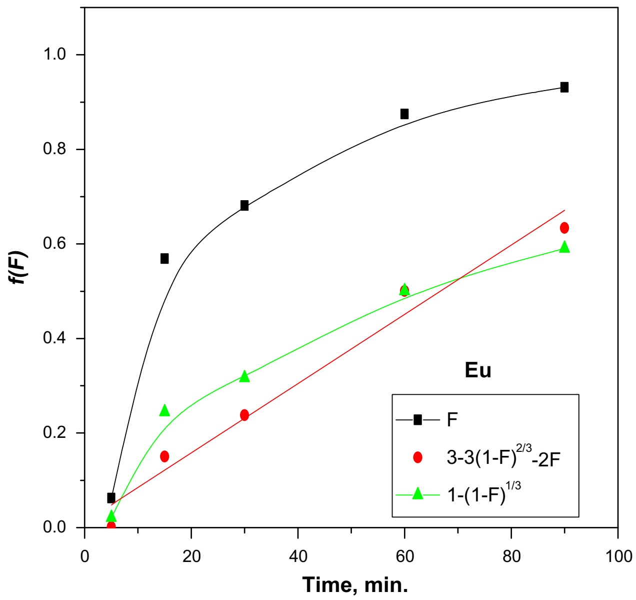

Fig. 21. Verification of the double shell model for Eu^{3+} adsorption.

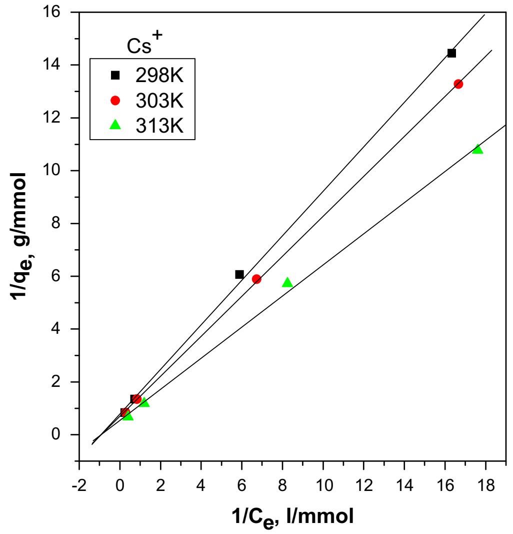

Fig. 22. Langmuir isotherm for Cs adsorption at different temperature.

The D–R isotherm model is applied for distinguishing between physical and chemical adsorption. The D–R isotherm model is applicable at low concentration ranges and can be used to describe sorption on both homogeneous and heterogeneous surfaces. The D–R isotherm model was given by the following equation:

$$\ln q_e = \ln q_m - \beta\varepsilon^2 \tag{15}$$

The plot of $\ln q_e$ vs. ε^2, straight lines were obtained for the adsorption of the ions, under study, as shown

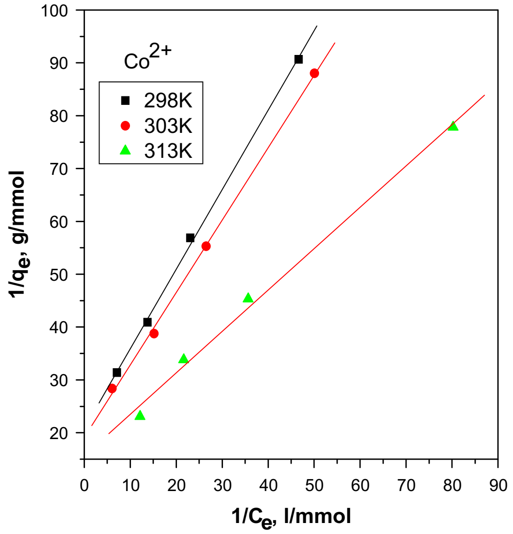

Fig. 23. Langmuir isotherm for Co adsorption at different temperature.

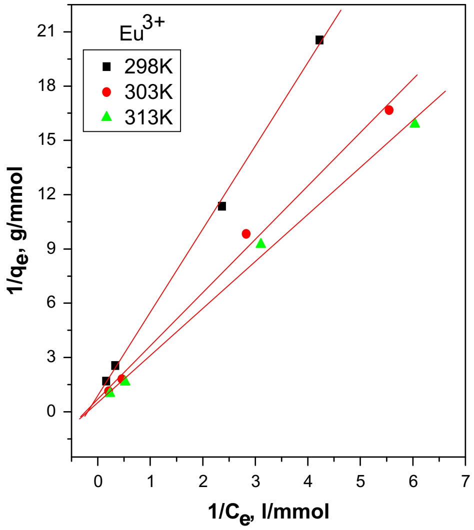

Fig. 24. Langmuir isotherm for Eu adsorption at different temperature.

in Figs. 28–30. The sorption capacity, q_m, (mmol/g), can be determined from the intercept and the value of the activity coefficient, β, (mol^2/kJ^2), was obtained from the slope, as illustrated in Table 7. The value of β is related to the adsorption mean free energy, E (kJ/mol), defined as the free energy change required to transfer one mole of ions from the infinity in the solution to the solid surface [25]. The relation is given as:

$$E = \frac{1}{\sqrt{2\beta}} \tag{16}$$

The mean free energy of adsorption, E, gives information about adsorption mechanism as chemical ion-exchange or physical adsorption. If E value is between 8 and 16 kJ/mol, the adsorption process is followed by a chemical ion-exchange [26,27], while if $E < 8$ kJ/mol, the adsorption is physical in nature [28].

From Table 7, the E values are between 8 and 16 kJ/mol for the three metal ions; therefore, the

Table 5
Langmuir isotherm parameters for the sorption of Cs^+, Co^{2+} and Eu^{3+}

Temperature (K)	298 K			303 K			313 K		
	Q (mmol/g)	b	R^2	Q (mmol/g)	b	R^2	Q (mmol/g)	b	R^2
Cs	1.26	0.93	0.998	1.44	0.99	0.998	1.60	1.06	0.998
Co	0.4	1.18	0.998	0.7	1.27	0.988	0.78	1.4	0.996
Eu	1.12	0.19	0.998	1.44	0.23	0.998	1.96	0.2	0.996

Table 6
Freundlich parameters for Cs^+, Co^{2+} and Eu^{3+} ions sorption as a function of temperature

Temperature (K)	298 K			303 K			313 K		
	1/n	log k	R^2	1/n	log k	R^2	1/n	log k	R^2
Cs	0.63 ± 0.03	−0.29 ± 0.03	0.994	0.68 ± 0.03	−0.21 ± 0.02	0.996	0.76 ± 0.04	−0.07 ± 0.03	0.992
Co	0.66 ± 0.03	−0.88 ± 0.05	0.990	0.69 ± 0.01	−0.77 ± 0.02	0.998	0.71 ± 0.02	−0.58 ± 0.03	0.996
Eu	0.78 ± 0.02	−0.81 ± 0.02	0.996	0.87 ± 0.02	−0.59 ± 0.02	0.996	0.79 ± 0.04	−0.50 ± 0.04	0.988

Table 7
D–R parameters for Cs^+, Co^{2+} and Eu^{3+} ions sorption as a function of temperature

Temperature	Cs				Co				Eu			
	β (mol^2/kJ^2)	q_m (mmol/g)	E (kJ/mol)	R^2	β (mol^2/J^2)	q_m (mmol/g)	E (kJ/mol)	R^2	β (mol^2/J^2)	q_m (mmol/g)	E (kJ/mol)	R^2
298 K	−0.005	0.920	10.00	0.988	−0.007	0.045	8.45	0.996	−0.0,061	0.489	9.05	0.992
303 K	−0.003	1.028	12.9	0.988	−0.0,054	0.049	9.62	0.988	−0.0,048	0.727	10.21	0.992
313 K	−0.0,025	1.518	14.14	0.999	−0.0,035	0.067	11.95	0.992	−0.0,031	1.079	12.70	0.993

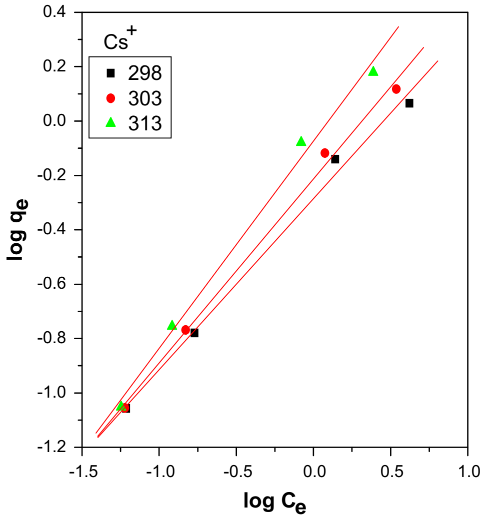

Fig. 25. Freundlich isotherm for Cs^+ adsorption at different temperature.

adsorption process is followed by chemical ion-exchange. The linear correlation coefficients for D–R models are shown in the Table 7, and are always greater than 0.98.

In order to gain insight into the thermodynamic nature of the sorption process, several thermodynamic parameters for the present systems were calculated. The Gibbs free energy change, ΔG, is the fundamental criterion of spontaneity. The reactions occur spontaneously at a given temperature if ΔG is a negative quantity. To calculate the different thermodynamic parameters, Van't Hoff equation was used which is given as follow [29]:

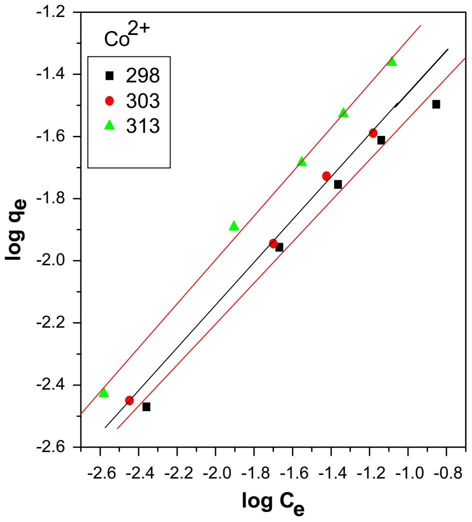

Fig. 26. Freundlich isotherm for Co^{2+} adsorption at different temperature.

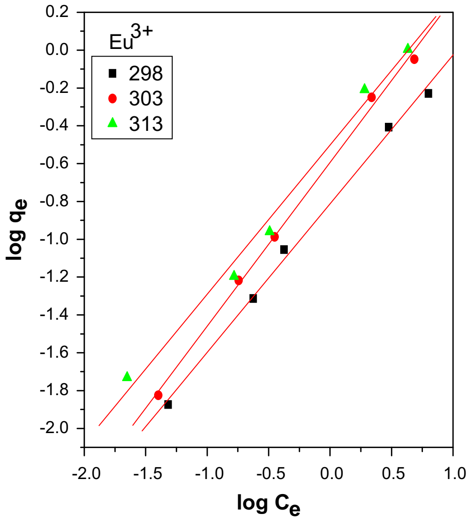

Fig. 27. Freundlich isotherm for Eu^{3+} adsorption at different temperature.

$$\Delta G = -RT \ln K_c \tag{17}$$

$$\Delta G = \Delta H - T\Delta S \tag{18}$$

$$\log K_c = -\frac{\Delta H}{2.303RT} + \frac{\Delta S}{2.303R} \tag{19}$$

where ΔG is the free energy, T is the absolute temperature in Kelvin, R is the general gas constant ($R = 8.314$ J/mol/K), ΔH is the enthalpy change, and

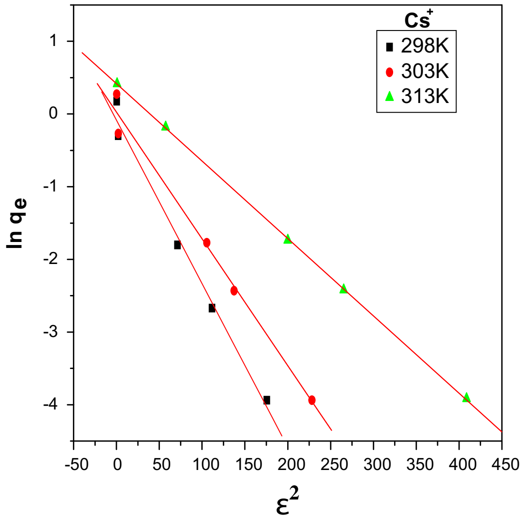

Fig. 28. D–R model for adsorption of Cs ion.

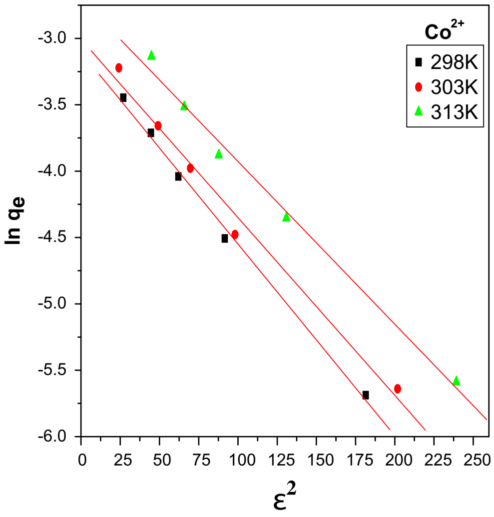

Fig. 29. D–R model for adsorption of Co ion.

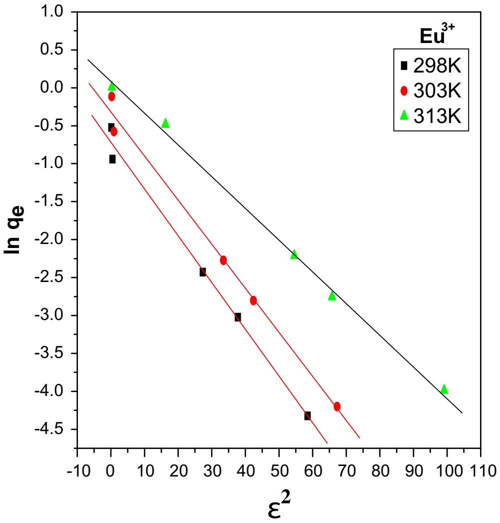

Fig. 30. D–R model for adsorption of Eu ion.

ΔS is the entropy change. Subsequently, the relation between log K_c and $1/T$ is given by Fig. 31. This figure shows a linear relation, the values of enthalpy change,

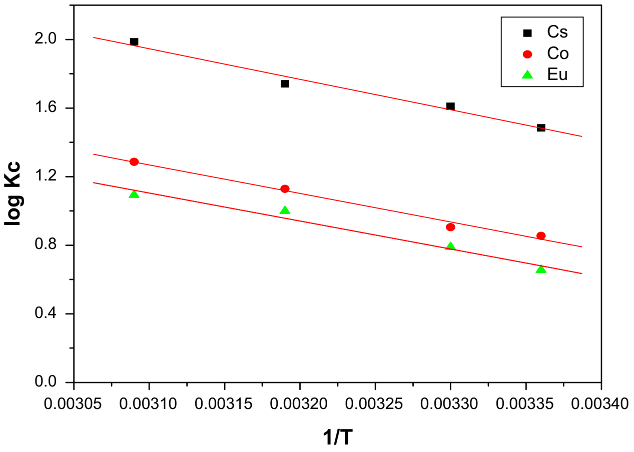

Fig. 31. Effect of temperature on sorption process.

Δ*H*, and entropy change, Δ*S*, can be calculated from the slopes and intercepts, respectively, as shown in Table 8. From these values, one can conclude that the positive values of enthalpy change, Δ*H*, for the three metal ions confirm the endothermic nature of the sorption process. The positive values of the entropy change, Δ*S*, show the increased randomness at the solid/solution interface with some structural changes in the adsorbate and adsorbent and an affinity of the poly-acrylonitrile-based cerium(IV) phosphate powder toward Cs^+ , Co^{2+}, and Eu^{3+} ions. The obtained negative values of free energy change, Δ*G*, confirm the feasibility of the process and the spontaneous nature of the sorption processes with preference toward Cs^+ than Co^{+2} than Eu^{+3}. Table 8 illustrates the K_c values that increase with increase in sorption temperature, thus implying a strengthening of adsorbate–adsorbent interactions at higher temperature. This also indicates that Cs^+, Co^{2+}, and/or Eu^{3+} ions considerably dehydrate.

4. Conclusion

Poly-acrylonitrile-based Ce(IV) phosphate is a well-behaved ion exchanger used for the sorption of Cs^+, Co^{2+}, and Eu^{3+}. The sorption process is controlled by

Table 8
Thermodynamic parameters for sorption process

Temperature (K)	K_c			Δ*H* (kJ/mol)			Δ*S* (J/mol/K)			Δ*G* (kJ/mol)		
	Cs^+	Co^{2+}	Eu^{3+}	Cs^+	Co^{2+}	Eu^{3+}	Cs^+	Co^{2+}	Eu^{3+}	Cs^+	Co^{2+}	Eu^{3+}
298	30.49	7.17	4.53	27.5	28.2	29.1	142.77	123.10	118.19	−8.467	−4.88	−3.743
303	40.64	8.05	6.15							−9.333	−5.254	−4.576
313	55.08	13.46	9.98							−10.432	−6.765	−5.987
323	96.83	19.31	12.38							−12.280	−7.951	−6.757

the particle diffusion process and obeys the pseudo-second-order mechanism. The obtained values of diffusion coefficient, D_i, were of the order of $10^{-12}\,m^2/s$ for Cs and Co ions and 10^{-13} for Eu ion, which indicates the chemisorption nature of the sorption process. The E values are between 8 and 16 kJ/mol for the three metal ions. Therefore, the adsorption process follows the chemical ion-exchange. The sorption has endothermic nature, which is indicated by the positive value of the enthalpy change. Thereby, the poly-acrylonitrile-based Ce(IV) phosphate can be used for the removal of the three metal ions from the waste solution.

References

[1] A.S. Kubo, D.J. Rose, Disposal of nuclear wastes: at an increased but still modest cost, more options can be explored and the outlook can be improved, Science 182 (1973) 1205–1211.

[2] C.I. Steefel, S. Carroll, P. Zhao, S. Roberts, Cesium migration in Hanford sediment: A multisite cation exchange model based on laboratory transport experiments, J. Contam. Hydrol. 67 (2003) 219–246.

[3] W.R. Gilmore, Radioactive Waste Disposal (Low and High Level), Noyes Data Corporation, New Jersey, NJ, 1977.

[4] S. Peterson, R.G. Wymer, Chemistry in Nuclear Technology, Addisson-Wesley Publishing Company, 1963.

[5] K.G. Varshney, Namrta Tayal, A.A. Khan, R. Niwas, Physicochem. Eng. Aspects 181 (2001) 123–129.

[6] M. Qureshi, K.G. Varshney, Inorganic Ion Exchangers in Chemical Analysis, CRC Press, Inc., Boca Raton, FL, 1991.

[7] M. Tsuji, S. Komarneni, Sep. Sci. Tech. 26 (1991) 644.

[8] M.J. Kang, B.S. Hahn, Adsorption behavior of aqueous europium on kaolinite under various disposal conditions, Korean J. Chem. Eng. 21 (2004) 419–424.

[9] Y.S. Ho, G. McKay, A kinetics study of dye sorption by biosorbent waste product pith, Resour. Conserv. Recycl. 25 (1999) 171–193.

[10] G. McKay, Y.S. Ho, The sorption of lead(II) on peat, Water Res. 33 (1999) 585–587.

[11] G. McKay, Y.S. Ho, Pseudo-second order model for sorption processes, Process Biochem. 34 (1999) 451–460.

[12] Yun Huang., Xiaoyan Ma, Guozheng Liang, Yongxia Yan, Shuhui Wang, Adsorption behavior of Cr(VI) on organic- modified rectorite, Chem. Eng. J. 138 (2008) 187–193.

[13] J. Crank, The Mathematics of Diffusion, Clarenden Press, Oxford, 1956.

[14] Xiaoyan Yang., Bushra Al-Duri, J. Colloid Interf. Sci. 287 (2005) 25–34.

[15] Ibrahim Kula., Mehmet Ugurlu, Hamdi Karaoglu, Ali C. Celik, Bioresour. Technol. 99 (2008) 492–501.

[16] G.E. Boyd, A.W. Adamson, L.S. Mayers, The exchange adsorption of ions from aqueous solutions by zeolites. II. Kinetics, J. Am. Chem. Soc. 69 (1947) 28–36.

[17] D. Reichenberg, J. Am. Chem. Soc. 75 (1953) 589.

[18] A.M. El-Kamash, A.A. Zaki, M. Abed El Geleel, J. Hazard. Mater. B127 (2005) 211–220.

[19] G.M. Walker, L.R. Weatherly, Kinetics of acid dye adsorption on GAC, Water Res. 33 (1999) 1895–1899.

[20] K.G. Scheckel, D.L. Sparks, Temperature effects on nickel sorption kinetics at mineral–water interface, Soil Sci. Soc. Am. J. 65 (2001) 719–728.

[21] A.M. El-Kamash, Evaluation of zeolite A for the sorptive removal of Cs^+ and Sr^{2+} ions from aqueous solutions using batch and fixed bed column operations, J. Hazard. Mater. 151 (2008) 432–445.

[22] L. Liberti, R. Passino, J.A. Marinsky, Y. Marcus (Eds.), Ion Exchange and Solvent Extraction, vol. 7, Marcel Dekker, New York, NY,. (Chapter 3) 1977.

[23] G. Schmuckler, S. Golstein, J.A. Marinsky, Y. Marcus (Eds.), Ion Exchange and Solvent Extraction, vol. 7, Marcel Dekker, New York, NY,. (Chapter 1) 1977.

[24] D. Mohan, K.P. Singh, Single and multi-component adsorption of cadmium and zinc using activated carbon derived from bagasse an agricultural waste, Water Res. 36 (2002) 2304–2318.

[25] S. Aksoyoglu, J. Radioanal. Nucl. Chem. 134 (1989) 393.

[26] A. Ozcan, A.S. Ozcan, S. Tunali, T. Akar, I. Kiran, Determination of the equilibrium, kinetic and thermodynamic parameters of adsorption of copper(II) ions onto seeds of *Capsicum annuum*, J. Hazard. Mater. B124 (2005) 200–208.

[27] F. Helffrich, Ion Exchange, McGraw Hill, New York, NY, 1962.

[28] M.S. Onyango, Y. Kojima, O. Aoyi, E.C. Bernardo, H. Matsuda, J. Colloid Interf. Sci. 279 (2004) 341–350.

[29] G.R. Choppin, A. Morgenstern, Thermodynamics of solvent extraction, Journal of Solvent Extraction and Ion Exchange 18 (6) (2000) 1029–1049.